HHS Public Access

Author manuscript

Am J Surg Pathol. Author manuscript; available in PMC 2016 October 01.

Published in final edited form as:

Am J Surg Pathol. 2015 October ; 39(10): 1313–1321. doi:10.1097/PAS.0000000000000469.

Frequent *FOS* Gene Rearrangements in Epithelioid Hemangioma: A Molecular Study of 58 Cases with Morphologic Reappraisal

Shih-Chiang Huang, MD[1,2], **Lei Zhang**[2], **Yun-Shao Sung**[2], **Chun-Liang Chen**[2], **Thomas Krausz, MD**[3], **Brendan C Dickson, MD**[4], **Yu-Chien Kao, MD**[5], **Narasimhan P Agaram, MBBS**[2], **Christopher D.M. Fletcher, MD, FRCPath**[6], and **Cristina R. Antonescu, MD**[2,*]

[1]Department of Pathology, Chang Gung Memorial Hospital, Chang Gung University, College of Medicine, Taoyuan, Taiwan

[2]Department of Pathology, Memorial Sloan Kettering Cancer Center, New York, NY

[3]Department of Pathology, University of Chicago, Chicago, IL

[4]Department of Pathology and Laboratory Medicine, Mount Sinai Hospital, Toronto, Ontario, Canada

[5]Department of Pathology, Shuang Ho Hospital, Taipei Medical University, New Taipei City, Taiwan

[6]Department of Pathology, Brigham and Women's Hospital, Boston, MA

Abstract

Epithelioid hemangioma (EH) is a unique benign vasoformative tumor composed of epithelioid endothelial cells. Although a small subset of EHs with atypical features harbor *ZFP36-FOSB* fusions, no additional genetic abnormalities have been found to date in the remaining cases. Based on a novel *FOS-LMNA* gene fusion identified by RNA sequencing in an index case of a skeletal EH with typical morphology, we sought to investigate the prevalence of *FOS* rearrangement in a large cohort of EHs. Thus 57 additional EH cases lacking *FOSB* rearrangements were studied for *FOS* gene abnormalities by FISH and results were correlated with morphologic appearance and clinical presentation. The EHs were subclassified as typical (n=25), cellular (n=21) and ALHE (angiolymphoid hyperplasia with eosinophilia)(n=12) variants. The ALHE was defined as an EH with a vascular ‘blow-out’ pattern associated with a variable degree of inflammation. There were 17 (29%) cases bearing *FOS* gene rearrangements among 58 cases tested, including 12 males and 5 females, with a mean age of 42 years. Most *FOS*-rearranged EHs occurred in the bone (10) and soft tissue (6), while only one case was cutaneous. The predominant anatomic site was the extremity (12), followed by trunk (3), head and neck (1), and penis (1). The incidence of *FOS* rearrangement was significantly higher in bone (59%, p = 0.006) and lower in head and neck (5%, p = 0.009). Twelve of the *FOS* rearranged cases were cellular EH (p = 0.001) associated with

*Correspondence to: Cristina R Antonescu, MD, Department of Pathology, Memorial Sloan Kettering Cancer Center, 1275 York Ave, New York, NY 10065; Phone number: 212-639-5905; Fax number: 212-717-3203; antonesc@mskcc.org.

Conflict of interest: none

moderate mitotic activity (2-5/10 HPF) and milder inflammatory background. All 12 ALHE cases lacked *FOS* gene abnormalities, suggesting different pathogenesis. In conclusion, *FOS* rearrangement was present in a third of EHs across different locations and histologic variants; however, it was more prevalent in cellular EH and intra-osseous lesions, compared to those in skin, soft tissue and head and neck. This genetic abnormality can be useful in challenging cases, to distinguish cellular EHs from malignant epithelioid vascular tumors. These results also suggest that dysregulation of the FOS family of transcription factors through chromosomal translocation is as a key event in the tumorigenesis of EH except for the ALHE variant.

Keywords

epithelioid hemangioma; angiolymphoid hyperplasia with eosinophilia; FOS; LMNA; VIM

Introduction

Epithelioid hemangioma (EH) is an uncommon but distinctive vascular neoplasm displaying well-formed vascular channels lined by prominent epithelioid endothelial cells [1-3]. As suggested from the variety of its previous designations, such as intravenous atypical vascular proliferation [4], angiolymphoid hyperplasia with eosinophilia (ALHE) [5, 6], inflammatory angiomatous nodule [7], and histiocytoid hemangioma [8], the morphologic spectrum of EH exhibits a wide range of appearances, including intravascular growth, a heavy inflammatory infiltrate, and a cellular/solid proliferation. Although initially described as having predilection for the skin and subcutis of the head and neck, further studies documented its ubiquitous anatomic location, involving deep soft tissue, bone, lymph nodes, lung, eye, colon, heart, spleen, and penis. [9] Due to its diverse histomorphologies the diagnosis of EH remains challenging, being confused at one end of the spectrum (ALHE) with other inflammatory conditions (e.g. Kimura disease), while at the other end of the spectrum (cellular EH) with malignant epithelioid vascular tumors, such as epithelioid hemangioendothelioma (EHE) and epithelioid angiosarcoma (AS). Moreover, the distinction from malignant lesions is further complicated by the aggressive clinical presentation of intra-osseous EH with destructive growth and/or multifocality, or by the presence of atypical histologic features with increased mitotic activity and necrosis [2, 3, 10].

Although our group has recently identified recurrent *ZFP36-FOSB* fusions in a small subset of EH with atypical features [10], the underlying genetic alteration responsible for most EHs remains elusive. In this study, we took advantage of an index case with available frozen tissue, which was subjected to RNA sequencing and FusionSeq analysis, to identify novel gene rearrangements. The gene fusion candidate was then validated and screened in a large set of EHs of various morphologic appearances and clinical presentations to determine its frequency and to evaluate genotype-phenotype correlations.

Materials and Methods

Patient Cohort and Pathological Classification

The study cohort of 58 EHs was collected from the archives of MSKCC Surgical Pathology files, the personal consultations of the senior authors (CRA, CDF) and Dr. Hsuan-Ying Huang (see Acknowledgement). All cases selected lacked FOSB gene abnormalities by FISH. The diagnostic criteria for EH included predominant epithelioid morphology of the endothelial cells, with moderate to abundant eosinophilic cytoplasm, and at least focal areas of overt vasoformative features. There was no frank endothelial multilayering nor significant cytologic atypia. The endothelial differentiation of epithelioid tumor cells was confirmed by CD34, CD31, and/or ERG immunohistochemistry in all cases. The EHs were further subclassified as typical, cellular and ALHE variants. The cellular EH were defined as having a solid growth in >50% of the tumor. EH characterized by distinct involvement of vessel wall with centrifugal growth and variable inflammatory infiltrate was categorized as ALHE variant [6]. The study was approved by the Institutional Review Board 02-060.

RNA Sequencing

Total RNA was extracted from the frozen tissue available in the index case by Trizol reagent (Invitrogen, Carlsbad, CA) and prepared for RNA sequencing in accordance with the standard Illumina mRNA sample preparation protocol (Illumina, San Diego, CA). Briefly, mRNA was isolated with oligo(dT) magnetic beads from total RNA (10 μg). The mRNA was fragmented by incubation at 94°C for 2.5 min in fragmentation buffer (Illumina). To reduce the inclusion of artifactual chimeric transcripts due to random priming of transcript fragments into the sequencing library because of inefficient A-tailing reactions that lead to self ligation of blunt-ended template molecules [11], an additional gel size-selection step (capturing 350-400 bp) was introduced prior to the adapter ligation step. The adaptor-ligated library was then enriched by PCR for 15 cycles and purified. The library was sized and quantified using DNA1000 kit (Agilent, Santa Clara, CA) on an Agilent 2100 Bioanalyzer according to the manufacturer's instructions. Paired-end RNA-sequencing at read lengths of 50 or 51 bp was performed with the HiSeq 2500 (Illumina). A total of about 38 million paired-end reads were generated, corresponding to about 3.8 billion bases.

Analysis of RNA Sequencing Results with FusionSeq Method

All reads were independently aligned with the STAR alignment software against the human genome sequence (hg19) and a splice junction library, simultaneously [12]. The mapped reads were converted into Mapped Read Format [13] and analyzed with FusionSeq [14] to identify potential fusion transcripts. Briefly, paired-end reads mapped to different genes are first used to identify potential chimeric candidates. A cascade of filters, each taking into account different sources of noise in RNA-sequencing experiments, was then applied to remove spurious fusion transcript candidates. Once a confident list of fusion candidates was generated, they were ranked with several statistics to prioritize the experimental validation. In these cases, we used the DASPER score (difference between the observed and analytically calculated expected SPER): a higher DASPER score indicated a greater likelihood that the fusion candidate was authentic and did not occur randomly.

Fluorescence In Situ Hybridization (FISH)

FISH on interphase nuclei from paraffin-embedded 4-micron sections was performed applying custom probes using bacterial artificial chromosomes (BAC), covering and flanking genes that were identified as potential fusion partners in the RNA-seq experiment. BAC clones were chosen according to UCSC genome browser (http://genome.ucsc.edu), see Supplementary Table 1. The BAC clones were obtained from BACPAC sources of Children's Hospital of Oakland Research Institute (CHORI) (Oakland, CA) (http://bacpac.chori.org). DNA from individual BACs was isolated according to the manufacturer's instructions, labeled with different fluorochromes in a nick translation reaction, denatured, and hybridized to pretreated slides. Slides were then incubated, washed, and mounted with DAPI in an antifade solution, as previously described [15]. The genomic location of each BAC set was verified by hybridizing them to normal metaphase chromosomes. Two hundred successive nuclei were examined using a Zeiss fluorescence microscope (Zeiss Axioplan, Oberkochen, Germany), controlled by Isis 5 software (Metasystems, Newton, MA). A positive score was interpreted when at least 20% of the nuclei showed a break-apart signal. Nuclei with incomplete set of signals were omitted from the score.

Reverse Transcription Polymerase Chain Reaction (RT-PCR)

An aliquot of the RNA extracted above from frozen tissue of the index case by Trizol Reagent (Invitrogen) was used to confirm the novel fusion transcript identified by FusionSeq. RNA quality was determined by Eukaryote Total RNA Nano Assay and cDNA quality was tested for *PGK* housekeeping gene (247 bp amplified product). Three microgram of total RNA was used for cDNA synthesis by SuperScript® III First-Strand Synthesis Kit (Invitrogen). RT-PCR was performed using the Clontech Advantage 2 PCR Enzyme System kit (Clontech, Mountain View, CA) for 33 cycles at a 65°C annealing temperature, using the following primers: *LMNA* intron 3 forward primer, 5′–CCATCAGACAAGTTAGGTCATAGGG–3′, and *FOS* exon 4 reverse primer, 5′–GATGCTCTTGACAGGTTCCACTG–3′. Amplified products were purified and sequenced by Sanger method after confirmed by gel electrophoresis.

Statistical Analysis

Statistical analysis was conducted using SPSS software (version 20; IBM, New York, NY). Associations between clinicopathological characteristics, histological variants, and *FOS* rearrangement were evaluated by using independent t, Pearson $\chi 2$, or Fisher exact tests according to the variable. Two-sided p values were calculated, and $p < 0.05$ was considered significant in all statistical analyses.

Results

Clinicopathologic Findings and Histologic Classification of EHs

The study cohort consisted of 35 men and 23 women with the mean age of diagnosis being 42 years (range, 14-81). The sites of involvement included the extremity (28, 48%), followed by head and neck (20, 34%), trunk (8, 13%), and penis (2, 3%). Within the extremities, there were 17 cases in the upper limb, including 5 cases involving the hands,

and 11 cases in the lower limb, with 9 cases involving the feet. Overall, the study included 10 cutaneous (17%), 31 soft tissue (54%), and 17 intra-osseous (29%) cases. Seven of the 10 cutaneous EHs occurred in a head and neck location, while two arose in the upper limb and one in the penis. Among 35 cases with available data, there were 7 patients presenting with multifocal lesions, 3 of them occurring in the bone.

The majority of cases were circumscribed and unencapsulated within a hemorrhagic background and hemosiderin-laden histiocytes. Most tumors had a distinctive lobulated growth, while 3 cases demonstrated a more infiltrative pattern with ill-defined borders. Two cases were entirely confined within a large-caliber muscular vascular lumen, indicating an intravascular location. The 58 cases were further divided into typical (25 cases, 43%), cellular (21, 36%) and ALHE (12, 21%). Increased mitotic activity (>1/10 HPF) occurred mostly in the cellular variant, but nuclear atypia and necrosis was observed in a subset of all variants. Marked inflammation with a prominent eosinophilic infiltrate was seen across all different histologic subtypes, including 5 typical, 2 cellular, and 9 ALHE variants. Among the 20 head and neck cases, 19 cases occurred in skin or superficial soft tissue and one in the mandible. Most head and neck EHs (75%) showed a moderate to marked inflammatory infiltrate.

A Novel *FOS-LMNA* Fusion in a Typical Variant of EH—The index case (EH1) was an intra-osseous EH resected from the 4th right rib of a 45 year-old man. Four years later he developed a soft tissue recurrence in the surgical bed of right chest wall, from which frozen tissue was available for RNA sequencing. Histologic examination of the recurrence was similar to that of the primary lesion and demonstrated a typical EH composed of lobules of immature or well-formed vascular structures lined by epithelioid endothelial cells (Fig. 1A and 1B).

The top fusion candidate identified by FusionSeq was an *FOS-LMNA* chimeric transcript (Fig. 2A). Reads alignment suggested a fusion between *FOS* exon 4 (chromosome 14q24.3) and *LMNA* intron 3 (chromosome 1q22). RT-PCR confirmed both the chimeric *FOS-LMNA* fusion (as predicted by the RNAseq fusion reads) and the reciprocal *LMNA-FOS* transcript. The *FOS-LMNA* transcript caused a stop codon immediately after the fusion junction (Fig. 2B). The expression of *FOS* gene was significantly increased in EHs compared to a group of other vascular and perivascular tumors (EHE, AS, and glomus tumors) with available RNAseq data (Fig. 2C). The EH1 index case had the highest *FOS* mRNA expression among EHs, including cases with *ZFP36-FOSB* or *WWTR1-FOSB* fusion, or EH lacking fusions. In contrast, other vascular tumors such as EHE, angiosarcoma, and glomus tumor did not demonstrate *FOS* up-regulation. We attempted to evaluate the significance of the stop codon following the breakpoint of the *FOS-LMNA* transcript and performed Western blotting on the EH1 index cases using the c-FOS rabbit polyclonal antibody directed to the N-terminal (Abcam, Cambridge, MA, #53036, 1:500). The EH1 showed a reduced level of the wild-type FOS (68 kDa) without evidence of an abnormal sized band. The control cases including other epithelioid vascular tumors (*FOSB*-positive EHa, *TFE3*-positive EHE, and one angiosarcoma) showed equal but higher wild-type FOS expression compared to EH1 index case (data not shown).

Subsequent FISH analysis, using a break-apart assay, showed rearrangements in both *FOS* and *LMNA* genes (Fig. 2D).

Clinical and Histologic Features of *FOS*-rearranged EHs

FISH analysis performed in the remaining 57 EHs identified a total of 17 cases (29%) with *FOS* gene rearrangements (Table 1), including 12 males and 5 females, with a mean age of 43 years (range 15-67). Most of the *FOS*-rearranged EH occurred in bone (10, 59%) and soft tissue (6), while only one was cutaneous, being a lesion on the penis. The predominant anatomic site affected was the extremities (12, 71%), with few examples in the trunk (3), head and neck (1), and penis (1). Histologically, 12 cases (70%) had increased cellularity and a solid growth pattern (Fig. 1C-G), corresponding to the cellular variant, while 5 were characterized by a typical histology (Fig. 1H). The only cutaneous *FOS*-rearranged EH involved the penis and showed an infiltrating pattern (Fig. 1I), while one cellular EH displayed intravascular growth (Fig. 1C). One cellular and one typical EH were associated with marked inflammation including eosinophils (Fig. 1G-H). Only one *FOS*-rearranged EH demonstrated focal necrosis. *FOS* rearrangements had a higher prevalence among the cellular type (57%, $p = 0.001$), intra-osseous location (59%, $p = 0.006$), lesions with minimal to mild inflammatory reaction (44%, $p = 0.023$), and lesions with moderately elevated mitotic activity (2-5/10HPF, 60%, $p = 0.004$), but was unrelated to the presence of necrosis, percentage of vacuolated cells, or eosinophilic infiltrate. Of the 10 patients with available follow-up data, 2 developed local recurrences at 7 months and 4 years after surgery, while the remainder were with no evidence of disease at last follow-up (mean 36.9 months, range 0.3-108 months).

All 12 cases with features of ALHE were negative for *FOS* rearrangement with 6 cases occurring in the head and neck, 5 cases in the extremities, and one case in the axilla. All except one case had moderate to marked inflammatory infiltrate with heavy eosinophilic component.

None of the remaining 57 cases showed the presence of an *LMNA* gene rearrangement by FISH. As FOSL1 and FOSL2 are members of the same family of FOS transcription factors, FISH for *FOSL1* and *FOSL2* gene abnormalities were performed in all EH cases that lacked *FOS* or *FOSB* rearrangements. However none of the 38 EH tested showed any gene alterations.

Rare *FOS-VIM* fusions are seen in intra-osseous cellular EH—As a previous intra-osseous EHE was reported to have a 46, XX, -6, t(10;14)(p13;q24) karyotype, involving the 14q24.3 locus where *FOS* gene is located [16], we hypothesized that it is likely this abnormality was identified in a cellular example of EH rather than an EHE. Thus we designed BAC probes spanning the 10p13 region and found two cases of *FOS*-rearranged EHs showing a break-apart signal in this region (Supplementary Table 1). Both cases were intra-osseous lesions, occurring in the foot of middle aged women (38 and 56 years-old, respectively) and microscopically were cellular EH lacking mitotic activity, nuclear atypia, and inflammatory reaction (Fig. 3A-3C). By FISH positional cloning [17], we further confined

the break within the *VIM* gene (Fig. 3D). Both patients were with no evidence of disease for 2 and 9 years, respectively, after surgery.

Discussion

While epithelioid vascular tumors ranging from benign EH to malignant EHE and AS share a common epithelioid endothelial morphology, they are distinct pathologic entities with different clinicopathological features and molecular alterations. Approximately 90% of EHE harbor the recurrent t(1;3)(p36;q25) translocation, resulting in a *WWTR1-CAMTA1* fusion [16], while a smaller subset have a t(x;11)(p11;q22) translocation, resulting in a *YAP1-TFE3* fusion [17, 18]. AS exhibits instead a more heterogeneous genetic profile, including *KDR* mutations limited to the breast location [19], and/or *MYC* amplification in most AS secondary to irradiation or chronic lymphedema, with or without *FLT4* co-amplification [20, 21]. About 35% of ASs harbor *PTPRB* or *PLCG1* mutations also mostly restricted to radiation-associated AS [22]. In our previous study, 20% of EH harbored *ZFP36-FOSB* fusions and one third of them demonstrated moderate nuclear pleomorphism and necrosis [10]. In that study *FOSB* rearrangements were seen in two-thirds of penile EHs tested, as well as in a small subset of bone and soft tissue lesions. Of interest, the majority of pseudomyogenic hemangioendotheliomas also harbor *FOSB* rearrangements, showing recurrent fusions with *SERPINE1* gene [23].

The terminology of EH has been controversial with some early reports suggesting that EH of bone represents a variant of EHE with metastasizing potential [24, 25]. However, subsequent studies disproved this notion and indicated that EH of bone, similar to EH of soft tissue or other anatomic locations, is a benign pathologic entity with a low recurrence rate [2, 3]. This concept is now more widely accepted and, as such, is reflected in the current WHO classification for soft tissue and bone tumors [9]. Nevertheless, the diagnosis of EH remains challenging, especially at the cellular/atypical end of the spectrum, where correct subclassification is often impeded by the lack of objective molecular markers. In the current study, we sought to further investigate molecular abnormalities in EH, by taking advantage of a case with available frozen tissue for RNA sequencing. The FusionSeq algorithm detected a novel *FOS-LMNA* gene fusion in the index case of an intra-osseous EH with typical morphology. The results were subsequently validated by RT-PCR and FISH. Further recurrent *FOS* gene rearrangements were then identified in 29% (17/58 cases) of EH tested, spanning a variety of anatomic locations and tissue planes (skin, soft tissue, and bone), suggesting a shared genetic abnormality across various clinical presentations. However, the incidence of *FOS* alterations was unevenly distributed, with EH of the head and neck having a significantly lower incidence (5%, 1/20 cases) compared to that in lesions of extremities (43%, 12/28), trunk (38%, 3/8) and penis (50%, 1/2 cases). Furthermore, the skeletal EHs had the highest incidence of *FOS*-gene rearrangement (59%, 10/17), compared to skin (10%, 1/10) and soft tissue (19%, 6/31). The only *FOS*-rearranged head and neck EH occurred in the superficial soft tissue; none of the 7 cutaneous lesions of head and neck showed *FOS* abnormalities by FISH. There was a significant correlation between the presence of *FOS* gene rearrangements and histologic variant of EH: none of the 12 EH cases displaying centrifugal growth from a muscular vessel had *FOS* gene abnormalities. This particular

histologic appearance is often seen in the head and neck or extremities, and was previously classified as ALHE by Fetsch et al [6], possibly indicating a different pathogenesis.

The *FOS* gene, known as FBJ murine osteosarcoma viral oncogene homolog and which maps to chromosome 14q24.3, belongs to the *Fos* gene family including *FOSB*, *FOSL1*, and *FOSL2* [26, 27]. The *FOS* gene encodes a transcription factor that can dimerize with members of the Jun family (c-Jun, JunB, and JunD), constituting the major components of the activating protein-1 (AP-1) complex. The AP-1 transcription factor binds to TPA-responsive elements (TREs; 5′-TGAC/GTCA-3′) of the promoter and enhancer regions of target genes, thereby regulating a wide variety of physiological and tumorigenic processes, including cell proliferation, tumor invasion, distant metastasis, and angiogenesis [26, 27]. c-fos stimulation triggers vascular endothelial growth factor-D (VEGF-D) overexpression, which in turn binds to the vascular and lymphatic receptors VEGFR-2 and VEGFR-3, causing tyrosine phosphorylation and, in human umbilical cord vein endothelial cells (HUVEC), activating proliferation, elongation, and branching to form an extensive network of capillary-like cords in three-dimensional matrix [28]. This angiogenic effect initiated by c-FOS-induced VEGF up-regulation has been implicated as an important mechanism for cancer progression and failure of peritoneal dialysis [29, 30]. The *LMNA* gene encodes lamin A and C that are structural protein elements of intranuclear peripheral thin filamentous meshwork, the nuclear lamina [31, 32]. Lamins have been considered key components of nucleoskeleton in maintaining nuclear structures and involving DNA replication and transcription and heterochromatin organization. *LMNA* gene rearrangements have been recently described in another mesenchymal tumor, being a 5′ fusion partner to *ALK* gene in an inflammatory myofibroblastic tumor [33].

The differential diagnosis of EH includes both EHE and AS. Especially, cellular EH, composed of large solid components, or EH with atypical histologic features, displaying necrosis and moderate cytologic atypia, are particularly challenging to distinguish from malignant epithelioid vascular tumors. Low power examination may reveal a lobular growth pattern and maturation of the vascular channel formation at the periphery of the lesion with conspicuous concentric layers of pericytes, which would favor a benign EH over other malignant diagnosis [3]. In contrast, EHEs are composed of characteristic strands or cords of epithelioid cells with abundant glassy eosinophilic cytoplasm and prominent cytoplasmic vacuolation, embedded in a distinctive chondromyxoid or hyalinized stroma. Importantly, most EHE lack well-formed vascular channels, and the only evidence of angiogenic properties is reflected by the so-called blisters cells, in the form of intra-cytoplasmic lumina [1-3, 9, 34]. The only notable exception is the *TFE3*-rearranged EHE, which shares with EH the presence of mature vascular lumen formation, but in contrast displays more significant cytologic atypia and diffuse and strong expression of TFE3 [18]. Furthermore, most epithelioid AS show significant cytologic atypia, with hyperchromasia and marked nuclear pleomorphism, which is absent in both cellular and atypical EH. Moreover, in contrast with EH, AS is characterized by infiltrative growth, with irregular anastomosing vascular channels, which are not present in EH [1-3, 9, 34]. This diagnostic challenge is further illustrated by the couple of reported cases in the cytogenetic literature, documenting 14q24.3 locus abnormalities (corresponding to the *FOS* gene locus), which are most likely in keeping

with a cellular/atypical EH rather than either EHE or AS [16, 35]. Based on such a previously reported case with t(10;14)(p13;q24) karyotype [16], we identified a novel *VIM-FOS* fusion in two intraosseous cellular EH cases by FISH positional cloning. The *VIM* gene, located at chromosome 10p13, encodes vimentin, a ubiquitous intermediate filament in mesenchymal cells. Along with microtubules and actin microfilaments, vimentin is part of the cytoskeleton and its overexpression may involve epithelial-mesenchymal transformation in cancer progression [36].

This study also sought to address the question whether ALHE, more commonly seen in the head and neck area and extremities, shares similar genetic abnormalities with other EH variants, which are more often seen in bone and soft tissue sites. In the large series by Fetsch et al [6], approximately half of the 96 EH cases examined were associated with prominent lymphoid follicles and damaged medium-sized vessels. This phenotype is prototypical of ALHE, first described by Wells and Whimster in 1969 [37], occurring predominantly in the subcutaneous tissue of the head and neck region. The key features of ALHE, including a prior history of trauma, lesional maturation over time, even capillary proliferation around a large vessel, the presence of vascular damage, and the extensive degree of inflammation, may suggest a reactive process, distinct from the neoplastic appearance of other EH variants. The distribution of ALHE also coincides with areas susceptible to injury, such as the head and neck and extremities. In the current study, all EH cases displaying a vascular ‘blow-out’ pattern, characteristic of ALHE, were devoid of *FOS* rearrangement, suggesting a different pathogenesis from classic and cellular EH.

In summary, we report novel and recurrent *FOS* gene rearrangements in nearly one third of EHs across a variety of locations and histologic variants. Of note, *FOS* abnormalities were present in half of the cellular EH variants and intra-osseous lesions. The *FOS* rearrangements are also much more common in the EH of extremities, trunk and penis, being seen in 40-50% of cases. In contrast, head and neck EHs are rarely affected by this genetic abnormality and all typical EH cases with centrifugal vascular involvement lack *FOS* rearrangement, suggesting that lesions previously designated as ALHE might represent a different pathologic entity.

Supplementary Material

Refer to Web version on PubMed Central for supplementary material.

Acknowledgments

We thank Dr. Hsuan-Ying Huang, from Kaohsiung Chang Gung Memorial Hospital, Taiwan, for his generous contribution of 18 cases.

Supported in part by: P01CA47179 (CRA), P50CA140146-01 (CRA), Cycle for Survival (CRA)

References

1. Fetsch JF, Sesterhenn IA, Miettinen M, et al. Epithelioid hemangioma of the penis: a clinicopathologic and immunohistochemical analysis of 19 cases, with special reference to exuberant examples often confused with epithelioid hemangioendothelioma and epithelioid angiosarcoma. Am J Surg Pathol. 2004; 28:523–533. [PubMed: 15087672]

2. Nielsen GP, Srivastava A, Kattapuram S, et al. Epithelioid hemangioma of bone revisited: a study of 50 cases. Am J Surg Pathol. 2009; 33:270–277. [PubMed: 18852673]
3. Errani C, Zhang L, Panicek DM, et al. Epithelioid hemangioma of bone and soft tissue: a reappraisal of a controversial entity. Clin Orthop Relat Res. 2012; 470:1498–1506. [PubMed: 21948309]
4. Rosai J, Akerman LR. Intravenous atypical vascular proliferation. A cutaneous lesion simulating a malignant blood vessel tumor. Arch Dermatol. 1974; 109:714–717. [PubMed: 4857233]
5. Castro C, Winkelmann RK. Angiolymphoid hyperplasia with eosinophilia in the skin. Cancer. 1974; 34:1696–1705. [PubMed: 4371945]
6. Fetsch JF, Weiss SW. Observations concerning the pathogenesis of epithelioid hemangioma (angiolymphoid hyperplasia). Mod Pathol. 1991; 4:449–455. [PubMed: 1924276]
7. Jones EW, Bleehen SS. Inflammatory angiomatous nodules with abnormal blood vessels occurring about the ears and scalp (pseudo or atypical pyogenic granuloma). Br J Dermatol. 1969; 81:804–816. [PubMed: 5359898]
8. Rosai J, Gold J, Landy R. The histiocytoid hemangiomas. A unifying concept embracing several previously described entities of skin, soft tissue, large vessels, bone, and heart. Hum Pathol. 1979; 10:707–730. [PubMed: 527967]
9. Fletcher, C.; Bridge, JA.; Hogendoorn, PC., et al. WHO Classification of Tumours of Soft Tissue and Bone. IARC; Lyon: 2013.
10. Antonescu CR, Chen HW, Zhang L, et al. ZFP36-FOSB fusion defines a subset of epithelioid hemangioma with atypical features. Genes Chromosomes Cancer. 2014; 53:951–959. [PubMed: 25043949]
11. Quail MA, Kozarewa I, Smith F, et al. A large genome center's improvements to the Illumina sequencing system. Nat Methods. 2008; 5:1005–1010. [PubMed: 19034268]
12. Dobin A, Davis CA, Schlesinger F, et al. STAR: ultrafast universal RNA-seq aligner. Bioinformatics. 2013; 29:15–21. [PubMed: 23104886]
13. Habegger L, Sboner A, Gianoulis TA, et al. RSEQtools: a modular framework to analyze RNA-Seq data using compact, anonymized data summaries. Bioinformatics. 2011; 27:281–283. [PubMed: 21134889]
14. Sboner A, Habegger L, Pflueger D, et al. FusionSeq: a modular framework for finding gene fusions by analyzing paired-end RNA-sequencing data. Genome Biol. 2010; 11:R104. [PubMed: 20964841]
15. Antonescu CR, Zhang L, Chang NE, et al. EWSR1-POU5F1 fusion in soft tissue myoepithelial tumors. A molecular analysis of sixty-six cases, including soft tissue, bone, and visceral lesions, showing common involvement of the EWSR1 gene. Genes Chromosomes Cancer. 2010; 49:1114–1124. [PubMed: 20815032]
16. He M, Das K, Blacksin M, et al. A translocation involving the placental growth factor gene is identified in an epithelioid hemangioendothelioma. Cancer Genet Cytogenet. 2006; 168:150–154. [PubMed: 16843105]
17. Errani C, Zhang L, Sung YS, et al. A novel WWTR1-CAMTA1 gene fusion is a consistent abnormality in epithelioid hemangioendothelioma of different anatomic sites. Genes Chromosomes Cancer. 2011; 50:644–653. [PubMed: 21584898]
18. Antonescu CR, Le Loarer F, Mosquera JM, et al. Novel YAP1-TFE3 fusion defines a distinct subset of epithelioid hemangioendothelioma. Genes Chromosomes Cancer. 2013; 52:775–784. [PubMed: 23737213]
19. Antonescu CR, Yoshida A, Guo T, et al. KDR activating mutations in human angiosarcomas are sensitive to specific kinase inhibitors. Cancer Res. 2009; 69:7175–7179. [PubMed: 19723655]
20. Manner J, Radlwimmer B, Hohenberger P, et al. MYC high level gene amplification is a distinctive feature of angiosarcomas after irradiation or chronic lymphedema. Am J Pathol. 2010; 176:34–39. [PubMed: 20008140]
21. Guo T, Zhang L, Chang NE, et al. Consistent MYC and FLT4 gene amplification in radiation-induced angiosarcoma but not in other radiation-associated atypical vascular lesions. Genes Chromosomes Cancer. 2011; 50:25–33. [PubMed: 20949568]
22. Behjati S, Tarpey PS, Sheldon H, et al. Recurrent PTPRB and PLCG1 mutations in angiosarcoma. Nat Genet. 2014; 46:376–379. [PubMed: 24633157]

23. Walther C, Tayebwa J, Lilljebjorn H, et al. A novel SERPINE1-FOSB fusion gene results in transcriptional up-regulation of FOSB in pseudomyogenic haemangioendothelioma. J Pathol. 2014; 232:534–540. [PubMed: 24374978]
24. Evans HL, Raymond AK, Ayala AG. Vascular tumors of bone: A study of 17 cases other than ordinary hemangioma, with an evaluation of the relationship of hemangioendothelioma of bone to epithelioid hemangioma, epithelioid hemangioendothelioma, and high-grade angiosarcoma. Hum Pathol. 2003; 34:680–689. [PubMed: 12874764]
25. Floris G, Deraedt K, Samson I, et al. Epithelioid hemangioma of bone: a potentially metastasizing tumor? Int J Surg Pathol. 2006; 14:9–15. discussion 16-20. [PubMed: 16501828]
26. Milde-Langosch K. The Fos family of transcription factors and their role in tumourigenesis. Eur J Cancer. 2005; 41:2449–2461. [PubMed: 16199154]
27. Durchdewald M, Angel P, Hess J. The transcription factor Fos: a Janus-type regulator in health and disease. Histol Histopathol. 2009; 24:1451–1461. [PubMed: 19760594]
28. Marconcini L, Marchio S, Morbidelli L, et al. c-fos-induced growth factor/vascular endothelial growth factor D induces angiogenesis in vivo and in vitro. Proc Natl Acad Sci U S A. 1999; 96:9671–9676. [PubMed: 10449752]
29. Yin Y, Wang S, Sun Y, et al. JNK/AP-1 pathway is involved in tumor necrosis factor-alpha induced expression of vascular endothelial growth factor in MCF7 cells. Biomed Pharmacother. 2009; 63:429–435. [PubMed: 19553068]
30. Catar R, Witowski J, Wagner P, et al. The proto-oncogene c-Fos transcriptionally regulates VEGF production during peritoneal inflammation. Kidney Int. 2013; 84:1119–1128. [PubMed: 23760290]
31. Fisher DZ, Chaudhary N, Blobel G. cDNA sequencing of nuclear lamins A and C reveals primary and secondary structural homology to intermediate filament proteins. Proc Natl Acad Sci U S A. 1986; 83:6450–6454. [PubMed: 3462705]
32. Schreiber KH, Kennedy BK. When lamins go bad: nuclear structure and disease. Cell. 2013; 152:1365–1375. [PubMed: 23498943]
33. Lovly CM, Gupta A, Lipson D, et al. Inflammatory myofibroblastic tumors harbor multiple potentially actionable kinase fusions. Cancer Discov. 2014; 4:889–895. [PubMed: 24875859]
34. Antonescu C. Malignant vascular tumors--an update. Mod Pathol. 2014; 27(Suppl 1):S30–38. [PubMed: 24384851]
35. Dunlap JB, Magenis RE, Davis C, et al. Cytogenetic analysis of a primary bone angiosarcoma. Cancer Genet Cytogenet. 2009; 194:1–3. [PubMed: 19737647]
36. Satelli A, Li S. Vimentin in cancer and its potential as a molecular target for cancer therapy. Cell Mol Life Sci. 2011; 68:3033–3046. [PubMed: 21637948]
37. Wells GC, Whimster IW. Subcutaneous angiolymphoid hyperplasia with eosinophilia. Br J Dermatol. 1969; 81:1–14. [PubMed: 5763634]

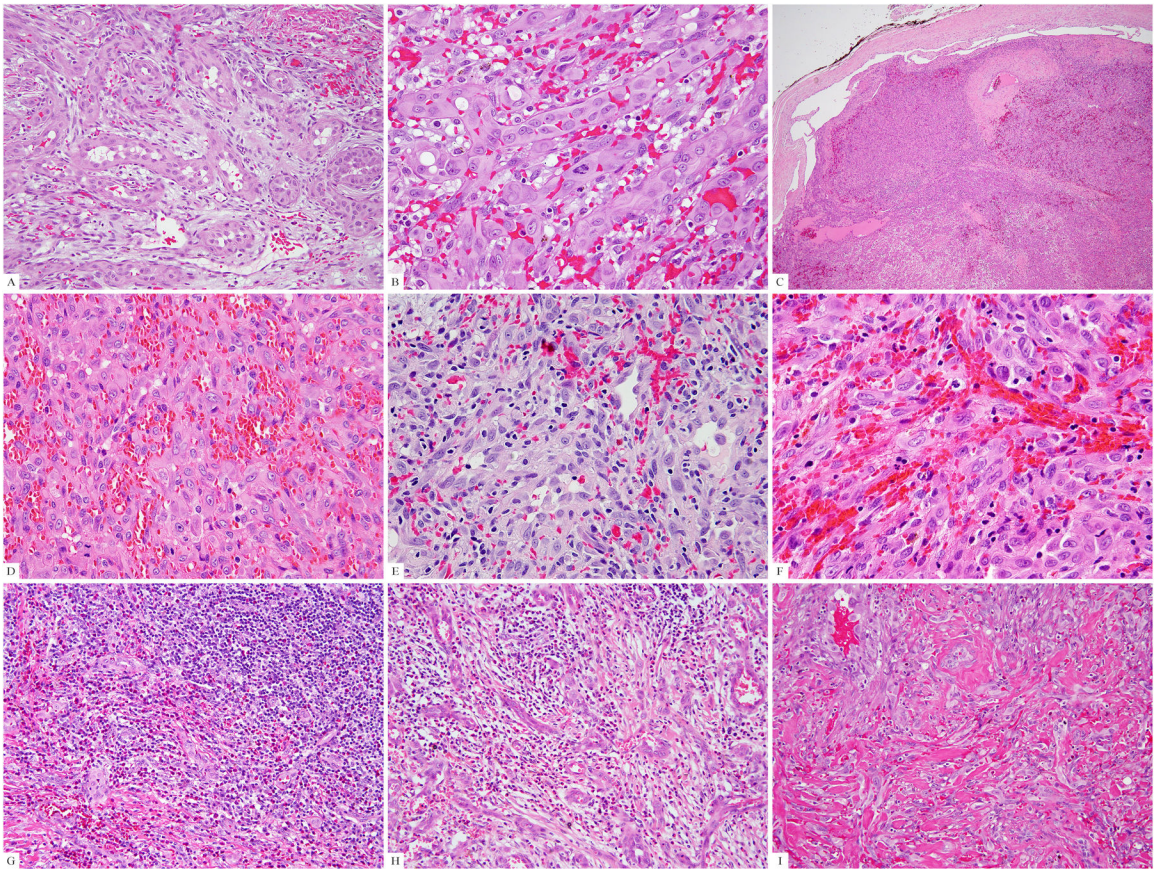

Figure 1. Pathologic findings of the *FOS*-rearranged EH cases

(A) The index case (case #1), positive for *FOS-LMNA* fusion, showed a typical morphology with epithelioid cells surrounding vascular lumina. (B) Lesional cells showed glassy eosinophilic cytoplasm with scattered vacuoles, vesicular nuclei, and prominent nucleoli (case #1). (C) One of the cellular EH (case #14) was confined to a dilated vascular channel, which at higher power (D) was composed of solid sheets of tumor cells. Cellular EH showed (E) variably prominent vascular spaces (case #12), (F) distinctive epithelioid cell features (case #11), and (G) surrounding lymphoid and eosinophilic infiltrates (case #13). (H) One typical EH was characterized by a prominent inflammatory background obscuring the proliferating vascular channels (H, case #15). Eosinophils were usually seen. (I) The penile EH (case #4) was composed of typical vasoformative structures but showed a more infiltrating growth pattern.

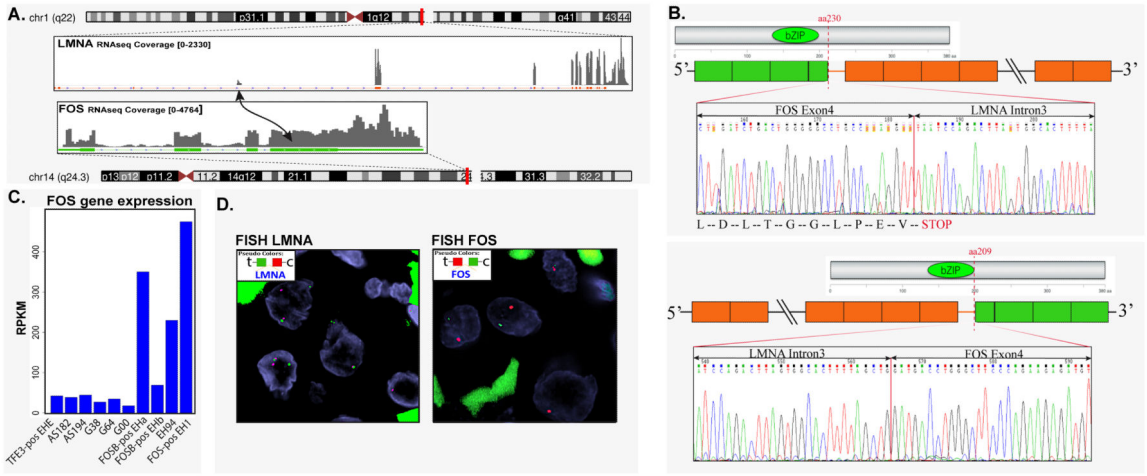

Figure 2. RNA sequencing and experimental validation of a novel *FOS-LMNA* gene fusion in a typical EH of bone (case#1)

(A) Schematic representation of RNA sequencing indicating the *LMNA* locus joined with the *FOS* gene, resulting in a t(1;14)(q22;q24.3) translocation. (B) RT-PCR confirmed both the *FOS-LMNA* and the reciprocal *LMNA-FOS* chimeric transcript. (C) FISH assay validated break-apart signals in both *FOS* and *LMNA* genes. (D) Normalized RNA sequencing read per kilobase per million mapped reads (RPKM) showed significant *FOS* mRNA upregulation in the index case (*FOS*-positive EH1), *FOSB*-rearranged cases (*FOSB*-positive EHa & EHb), and a fusion-negative EH (EHc), compared to epithelioid hemangioendothelioma (EHE), angiosarcoma (AS), and glomus tumor (G).

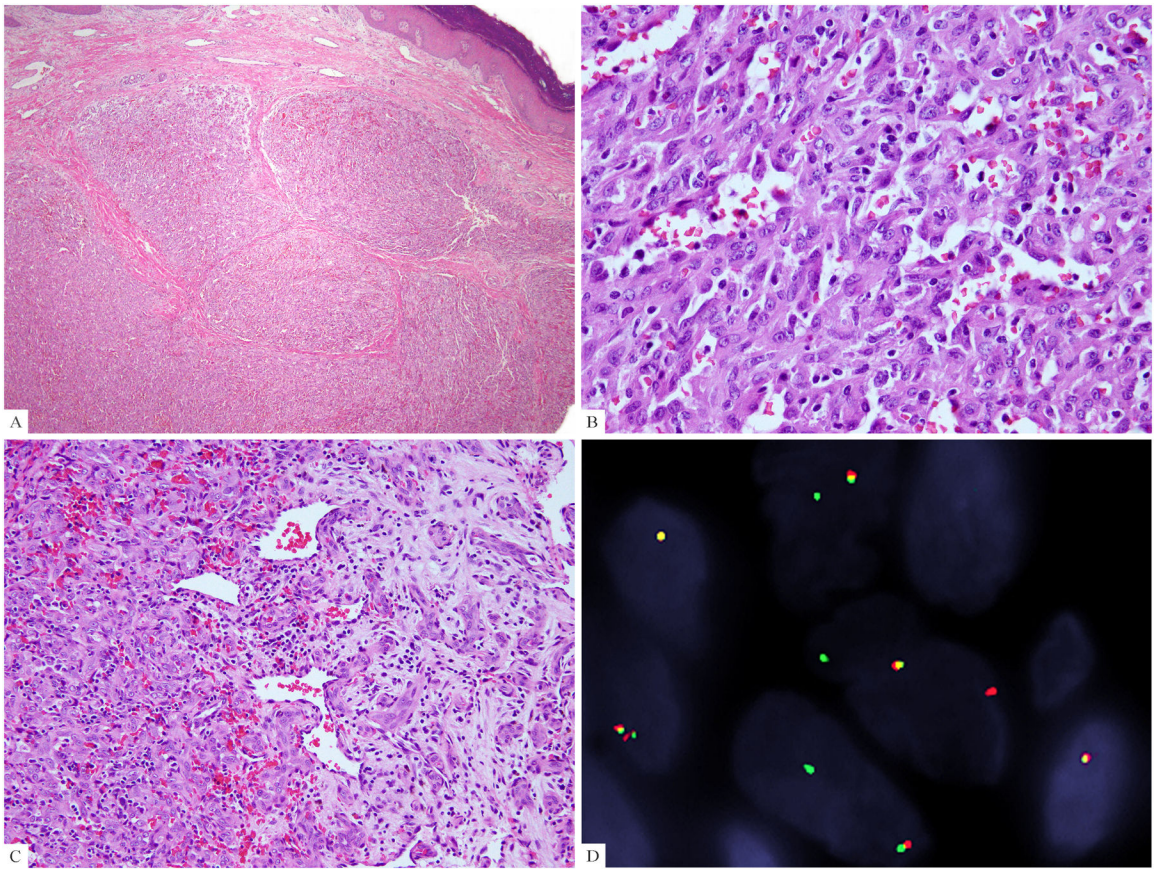

Figure 3. Histologic features of cellular EHs harboring *FOS-VIM* fusion

(A) The intraosseous cellular EH (case #2) extended to the skin and showed a distinctive lobulated growth. (B) Higher magnification demonstrated solid sheets with scattered vascular channels. (C) Transition between central solid growth and peripheral maturation into well-formed vascular structures was identified (case #3). (D) *VIM* break-apart signals by FISH assay (case#2).

Table 1

The clinicopathologic features of *FOS*-rearranged epithelioid hemangioma

Case	Age/Sex	Depth	Location	Multifocal	Histologic variant	Genetic alterations
1	45/M	Bone	Rib	No	Typical	*LMNA-FOS*
2	56/F	Bone	Foot	Yes	Cellular	*VIM-FOS*
3	38/F	Bone	Foot (cuboid)	NA	Cellular	*VIM-FOS*
4	48/M	Cutaneous	Penis	Yes	Typical	*FOS* rearrangement
5	63/M	Soft tissue	Arm	No	Cellular	*FOS* rearrangement
6	31/M	Bone	Foot	No	Cellular	*FOS* rearrangement
7	38/M	Soft tissue	Arm	No	Typical	*FOS* rearrangement
8	23/M	Bone	Chest wall	No	Typical	*FOS* rearrangement
9	41/M	Bone	L5 vertebra	No	Cellular	*FOS* rearrangement
10	67/M	Soft tissue	Scalp	NA	Cellular	*FOS* rearrangement
11	46/F	Bone	Metatarsal	NA	Cellular	*FOS* rearrangement
12	45/F	Soft tissue	Foot	NA	Cellular	*FOS* rearrangement
13	54/M	Soft tissue	Arm	NA	Cellular	*FOS* rearrangement
14	67/F	Soft tissue	Hand	NA	Cellular	*FOS* rearrangement
15	15/M	Bone	Toe	No	Typical	*FOS* rearrangement
16	15/M	Bone	Femur	No	Cellular	*FOS* rearrangement
17	18/M	Bone	Radius	No	Cellular	*FOS* rearrangement

NA: not available